Analysis of VLF-EM Data for Potential Cassiterite Mineralization Delineation Zone in Rafin-Bareda Area North-Western Nigeria

Micah Adamu[1], Nasir K Abdullahi[1] and Dogara D Matoh[1]

[1] Department of Physics, Faculty of Science, Kaduna State University, Kaduna State, Nigeria

Corresponding E-mail: nasir.abdullahi@kasu.edu.ng

Abstract

VLF-EM geophysical technique was employed to delineate potential cassiterite mineralization at Rafin Bareda, Dutsen-Wai, Kubau Local Government area of Kaduna state, North Western, Nigeria. A total area of 3.025 km2 was covered along eleven (11) traverses separated by 25m with a measurement interval of 10m taken in the East-West direction. The response of the in-phase component revealed various anomalous zones while Fraser-filtered plots of the in-phase peaked over the anomalous zones and the Karous-Hjelt filtered response of the in-phase correlates quite well with the results of the Fraser filtered data. In order to achieve the aim of the investigation, and since the VLF data was collected in the magnetic mode, enhancement procedures such as reduced to equator and analytical signal techniques were applied to the Fraser Filtered response of the In-phase component and correspondingly, Center for Exploration Targeting (CET), Source Parameter Imaging and Euler Deconvolution algorithms of the Oasis Montaj were successively employed to delineate potential mineralization zones and best locations for drilling productive cassiterite in the study area. Enhanced maps show linear features trending in the NE-SW and NW-SE directions with minor traces in the N-S direction. Most of the delineated zones of high analytical signal signature were either intercepted or flanked by the extracted lineament which is indicative of positive correlation between the extracted lineament and the high amplitude response of the analytical signal and also, validated the occurrence and positioning of the cassiterite mineral deposits is greatly controlled by the lineament system across the study area and the development of conductive zones of high apparent current with positive values reflects inferred subsurface structural fractures and/or mineralized zones. Depths evaluation analysis from the Euler Deconvolution (ED) technique using structural index of 1, ranged from 5 m to 15 m while depths varying from 4.9 m to 13.7 m were obtained from the Source parameter imaging technique.

Keywords: Cassiterite; Fraser Filter; Karous-Hjelt Filter; Conductor; Euler deconvolution.

I. INTRODUCTION

Nigeria is endowed with vast but untapped solid economic minerals such as gold, cassiterite, columbite, Tantalite etc., consequently, a lot of mining activities (formal and informal) is being carried out over many years in the study area [1, 2]. Cassiterite (SnO2) is the sole source of tin and about 80% of tin ore in Nigeria are from secondary deposits found in downstream (tin placer deposit) derived primarily

from tin lodes or veins and granitic rocks [3]. Reference [4] referred to the Younger Granite Tin Province as Younger Tin field of Nigeria and the Younger Granite provinces in Nigeria include Dutsen-Wai, Nok, Kudaru, Jama'a, Richi, Pankshin, Amo, Keffi, and Jos in the North Western and North central parts of Nigeria. The most active tin mining in Nigeria especially Rafin Bareda (Dutsen-Wai) have being carried out by the using trial and error means with the aim to meet individual financial needs not minding the environmental degradation impact on the host community (Fig. 1). The Very low frequency electromagnetic (VLF-EM) geophysical method is known for quick mapping of subsurface structures/conductors and also more reliable [5] and can be simultaneously used for environmental and minerals exploration investigation. The VLF-EM method has been successfully applied for detection of basement fractures favorable to uranium mineralization [6, 7] and mapping of suspected gold mineralization [8]. The aim of the present study is to delineate cassiterite mineralization zones in the study area through the application of Very Low Frequency (VLF-EM) method.

Fig. 1 Local Separation of the Cassiterite from the gravel sand

A. Geology and location of the study area
The study area is Dutsen-Wai (Fig 2.) situated in the northern part of Kaduna state bounded by Latitude 10^0 51'.480", $10^0$51'.500" N and Longitude $8^0$12'.50", $8^0$13'.20" E. The study area is 6.3km2 within the Younger Granite Ring and has a lot of natural resources such as iron ore, tin ore etc. The study area is accessible by road from neighboring states. The origin of the Younger Granite Ring complex in Nigeria is often referred to as being an orogenic [9]. The Basement complex in the study area is intruded into homogenous amphibiotic grade basement composed of migmatite and granite gneisses [10]. Three basic igneous units (Volcanic, Biotite granite and Albite riebeckite granite in sequential order) common to the younger granite suite make up the exposure and exhibit sharp mutual

contacts [11, 12]. The biotite granite is the main source of the tin deposits mined on a very small scale in the area and it is highly heterogeneous in appearance but with the same formation except in the degree of late stage albitization [12]; contact with the basement rocks to the east are poorly defined and the sequence of extrusive and intrusive igneous events in the province are well documented [13]. In Dutsen-Wai complex in particular, the emanated outcrop limits give the probable extent of the associated initial ring fracture. Ring fracture followed by cauldron subsidence is considered to be the major mode of intrusive emplacement for the younger granites and is thought to give rise to plutons roughly circular in plan with generally steeply dipping contacts [11], [13] and [12]. Also, Older Basalts, laterized older Basalts and newer Basalts preserve alluvial cassiterite deposits [14, 15].
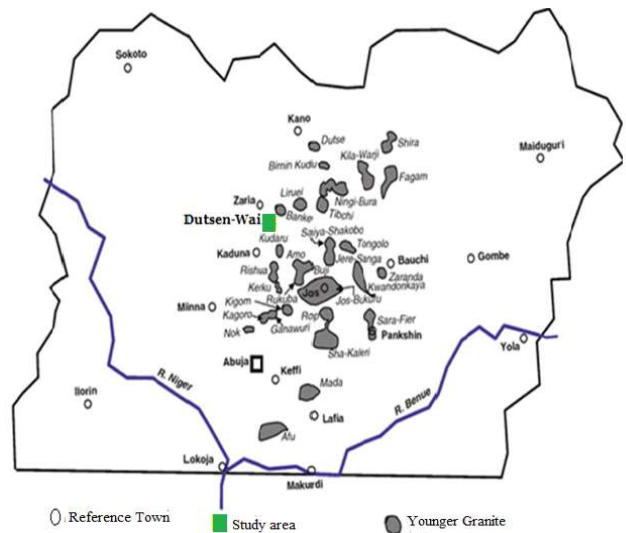

Fig. 2 Major younger granite localities in Nigeria [9]

II. MATERIALS AND METHODS

A. Materials
VLF-EM data in the East-West direction were collected along eleven traverses in the study area with the Scintrex ENVI System equipment to measure magnetic components. A transmitter located at Rosny, France operating at a frequency of 19.1 kHz with coordinates N46^0 42'.26", E$001^0$14'.89" was used as suitable frequency because it provides the EM field which approximates parallel to the traverse direction of the strike of the envisaged geological structure beneath the ground surface. The Universal Transverse Mercator (UTM) coordinate system was used and the lengths of the profiles range from 1000 m to 1040 m. The in-phase and quadrature data were presented as single profiles.

B. Methods
1) VLF-EM Measurements
The VLF method which the present work adopted allows for mapping of electrical conductors without contact with the

ground and it is conveniently used for investigation over wide area and has been often used to help in mapping of geological structures for the past four (4) decades [16]. The techniques utilize the incoming signal radiating from military navigation radio transmitter operating at cut-off frequencies of 15-30 kHz. The VLF method generally yields considerable EM anomalies, even over poor conductors such as sheared contacts, fracture zones, and faults, hence, this method has been the most popular tool for the rapid mapping of near-surface geological structures [17], [18], [19] and [20]. The principle of VLF-EM survey is based on the fact that the ratio of the secondary vertical magnetic component to the horizontal primary magnetic field is a measure of conductivity/resistivity contrast since this tipper component is of internal origin of the anomalous body [21]. The magnetic component of the VLF wave is mainly used for field measurement. According to the basic EM theory, the primary EM field is shifted in phase when encountering a conductive body and the conductive body then becomes the source of a secondary field. The VLF instrument detects the primary and secondary fields, and separates the secondary field into in-phase and quadrature components based on the phase lag of the secondary field. These two components of the secondary field are sometimes referred to as the tilt (in-phase) and ellipticity (quadrature). When the VLF-EM method is used for geophysical survey, the in-phase response is sensitive to metal or good conductive bodies. The quadrature response, on the other hand, is sensitive to the variation of the earth electrical properties [22]. To locate the anomalies, measured data were processed using Fraser filtering while current pseudo depth sections were produced through the Karous–Hjelt filtering procedure for semi-quantitative interpretation. The linear filtering technique developed by [23] transforms non-contourable in-phase data to contourable form. The filtering process simply involves running a four-point weighted average using the weights of -1, -1, +1, -1. This simple digital filter operator passes over the in-phase component and when plotted generally peaks over the top of the conductor. This alteration of the raw data can be summarized in two statements: (a) the filter phase shifts all spatial frequencies by 90^0, i.e., it turns crossovers into peaks or troughs; and (b) it exhibits a band pass response, in other words, it greatly diminishes either sharp irregular responses (noise) or long rolling responses. At the same time, it accentuates responses which are the nearest to the filter's shape [24]. The Karous–Hjelt filter technique is a more generalized and rigorous form of the Fraser filter but is directly derived from the concept of magnetic fields associated with current flow in the earth. The filter provides a pictorial indication of the depths of various current concentrations and hence the spatial distribution of subsurface geological features [25]. Over conductors, the in-phase part of the equivalent current distribution has only positive values. Negative parts on both sides of the conductor

can be caused either by the length of the filter or by the decrease in current density due to current gathering which is not present in 2-D structures [26]. A number of filters with various lengths and shapes can be developed, however, the optimized Hjelt filter [27] is expressed as:

$$\frac{\Delta z}{2\pi} I_a(0) = 0.102 H_{-3} - 0.059 H_{-2} + 0.561 H_{-1} -$$
$$0.0561 H_1 + 0.059 H_2 + 0.102 H_3 \qquad (1)$$

Where $I_a(0) = 0.5 \left[I \left(\frac{\Delta x}{2} \right) + I \left(-\frac{\Delta x}{2} \right) \right]$ and H_{-3}, H_{-2} etc., are measure data at consecutive stations. Δx is the data point interval and I_a is apparent current density value. The estimated depth to the top of the subsurface geological structure.

2) Reduction to Magnetic Equator (RTE)

In order to remove any possible cultural noise as well as interpretation ambiguity associated with low latitude effect which makes the peaks of anomalies to be wrongly or improperly positioned over corresponding sources and skewed along a particular direction in addition, reduction to magnetic equator filter (RTE) was applied to the Fraser filtered of the In-phase component since the study area is situated in low latitude. This method uses the Geosoft Oasis Montaj magma tool® to apply the RTE filter with calculated declination and inclination of -0.2^0 and -1.9^0 respectively.

3) Analytical Signal (AS)

For the delineation of edges of similar magnetic responses which may coincide with lithological boundary, the analytical signal filtering was performed. It is a vector sum of the three orthogonal derivatives (horizontal gradient (HDR) in the x-direction and in y-direction, and vertical gradient (VDR) as stated in (2) (where T is the total magnetic field) and its amplitude peaks over magnetic boundaries.

$$|A(x,y)| = \sqrt{\left(\frac{\partial(\Delta T)}{\partial x} \right)^2 + \left(\frac{\partial(\Delta T)}{\partial y} \right)^2 + \left(\frac{\partial(\Delta T)}{\partial z} \right)^2} \qquad (2)$$

4) Source Parameter Imaging (SP)

The use of Source Parameter Imaging or SPI technique in the determination of depth to magnetic sources is known [28]; [29]; and [30]. It is a profile or grid-based method for estimating magnetic source depths, and works for two models: a dipping thin dike and a sloping contact. The local wavenumber (k) has maxima located over isolated contacts and depths can be estimated without assumptions about the thickness of the source bodies. Solution grids using the SPI technique show the edge locations, depths, dips, and susceptibility contrasts. The method utilizes the relationship between source depth and the local wavenumber (k) of the observed field, which can be calculated for any point within a grid of data via horizontal and vertical gradients. For the dipping contact, the maxima of k are located directly over the isolated contact edges and are independent of the magnetic

inclination, declination, dip, strike and any remnant magnetization. The depth as reported by [31] is estimated at the source edge from the reciprocal of the local wavenumber, as follows:

$$\text{Depth}_{(x=0)} = \frac{1}{k_{max}} \qquad (3)$$

Where k_{max} is the peak value of the local wave number k over the step source. One more advantage of this method is that the interference of anomaly features is reducible, since the method uses the second order derivatives. The theory of SPI method for depth estimates can be found in [26] and [29].

5) Euler Deconvolution

Euler deconvolution technique used to determine depth and location of features that represent structures, is based on Euler's homogeneity equation;

$$(x - x_0)\frac{\partial M}{\partial x} + (y - y_0)\frac{\partial M}{\partial y} + (z - z_0)\frac{\partial M}{\partial z} = -NM \quad (4)$$

Where $\frac{\partial M}{\partial x}$, $\frac{\partial M}{\partial y}$ and $\frac{\partial M}{\partial z}$ represent first order derivative of the magnetic field along x, y and z directions respectively. N is the structural index which is related to the geometry of the magnetic source. N = 1 which represent a dyke was used as the structural index. The homogeneity equation relates magnetic field to the location and depth of its sources with the equation. The VLF-EM data collected were subjected to the Euler deconvolution method to locate the source of the cassiterite mineralization field based on both amplitude and gradients employing the Oasis Montaj software®.

III. RESULTS AND DISCUSSION

Fig. 3 shows the raw data of both In-phase and Quadrature components as well as the Fraser filtered response of the in-phase component along profile A. The in-phase data varies from -11.6 % to 11.4 % and shows several cross-overs with the horizontal axis, with two prominent negative peaks at the 490 m and 810 m profile distance with peak-peak amplitude of -15.8 % and 11.6% respectively. The Quadrature component at these cross-overs shows negative inflection with amplitude of 9.9 % and 11.6 % respectively which may indicate a good conductor in a weakly conductor [35]. The quadrature component varies from -14.5% to 12.5%. The Fraser filtered of the In-phase component shows a high amplitude signal which is symmetrical at profile distance $500\ m$ suggestive of an anomalous body of large dimension and steeply dipping source. The asymmetry of the Fraser responses at other profile distances suggest that the conductive structures are also from dipping sources. The broad amplitude with low frequency ($14.4\ \%$ at $410\ m$) indicates deeper sources. The Karous-Hjelt plot (Fig.4) reveals the pictorial view of the spatial distribution of current density with pseudo-depth and it can be seen that the points of positive peaks in the Fraser filtered response correspond to the positive current densities while the negative peaks revealed negative current densities. This observed trend was exhibited by most of the remaining profiles B to K (Figures 5, 6, 7 and 8).
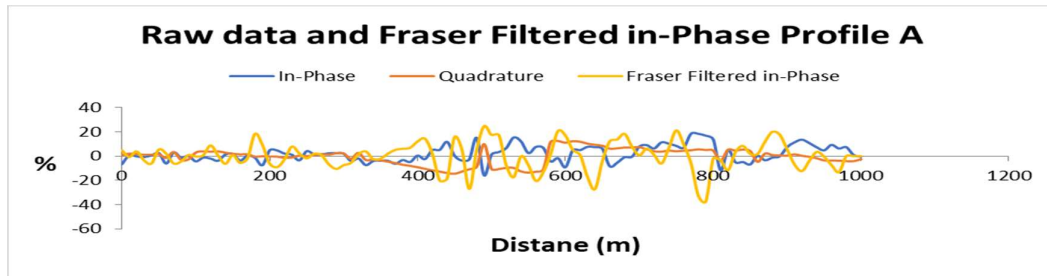

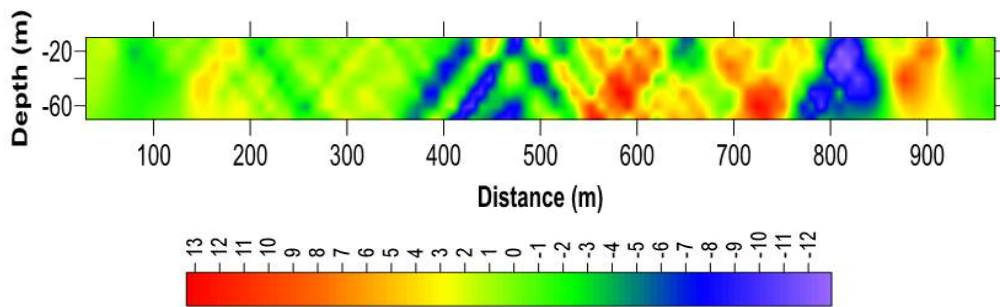Fig. 3 In-phase, Quadrature and Fraser Filtered of In-phase components along profile A

Fig. 4 Current density cross-section plot of real component along profile A
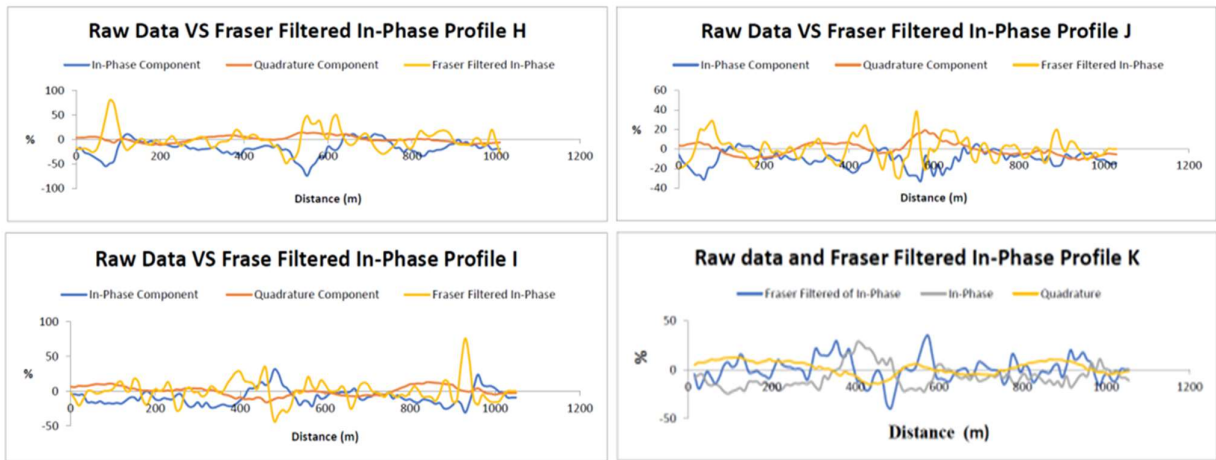
Fig. 5 Stacked map Profiles B-G

Fig. 6 Stacked map of Profiles H-K

Fig. 9 is the map of the raw data of the in-phase components of the 11 traverses in the study area depicting both positive and negative values in a bipolar way ranging from +0.876 to +19.93 % and -30.84 to -0.029% respectively. Fig. 10 show both the reduced to equator (RTE) response of the Fraser filtered of the in-phase component (a) and the Karou-Hjelt filter (b) of the study area with striking similarities and exhibiting linear features trending in the NE-SW and NW-SE directions with variable amplitudes which correspond to the structural trends of the basement complex of Nigeria [36] and [37]. These linear features (covering magenta, red, deep yellow and green colors) delineating different features of varying degrees of conductivity correspond with the cross overs observed in the In-phase component and are inferred fractures and/or mineralized zones in the study area. The broader and thin anomalies observed both in the Fraser filtered and the Krous-Hjelt filtered responses could be attributed either to the fact that the quartz vein is not continuous or it is inclined as a result of the depths being controlled by the depth of the conductive body to the surface and the attitude of the study area. According to [8], the negative real component value anomaly is usually associated with massive barren quartz vein with no gold mineralization.
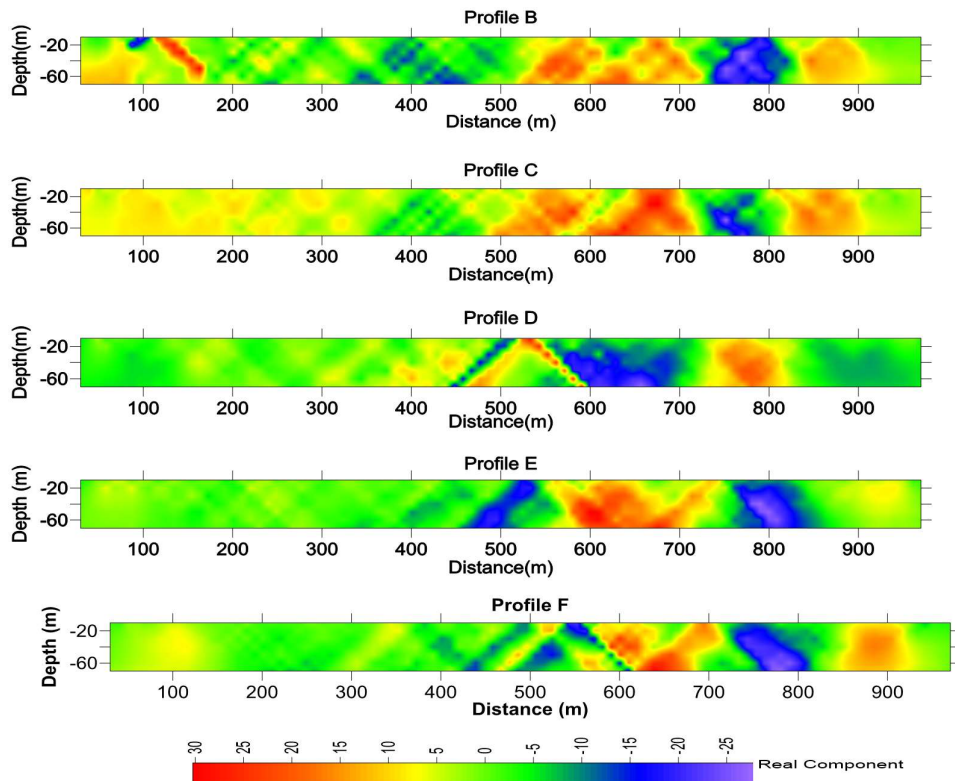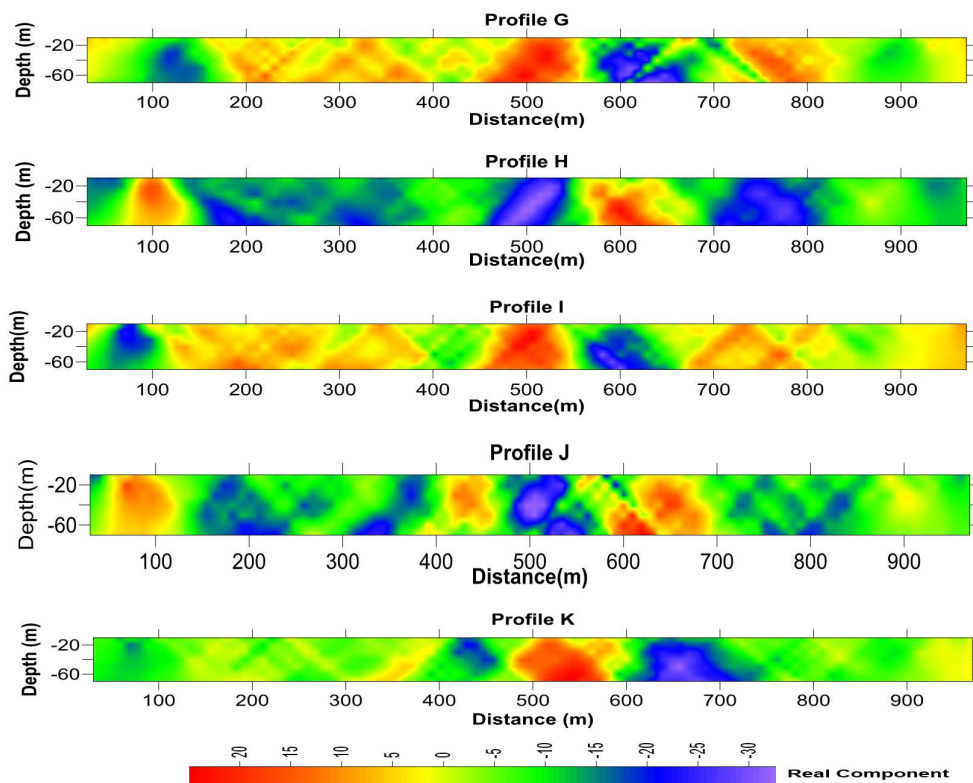
Fig. 7 Staked map of Karous-Hjelt (B-F) profiles

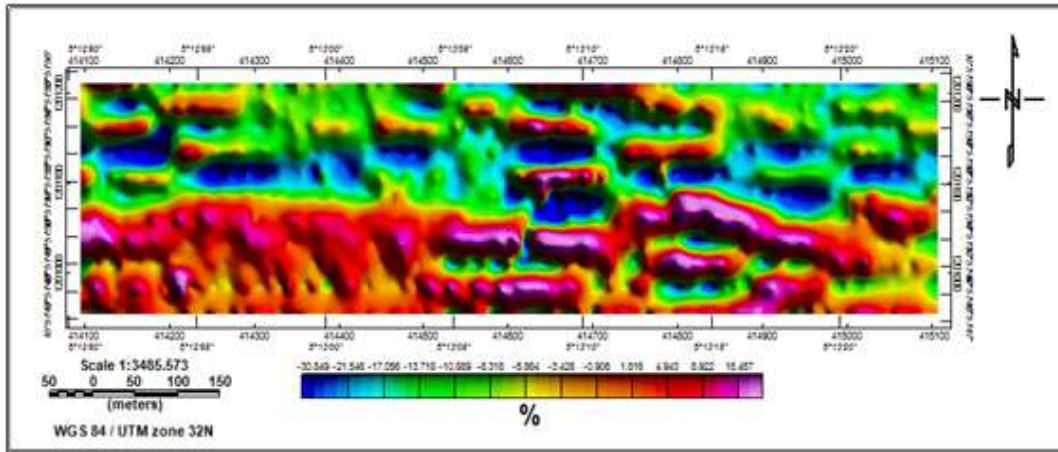Fig. 8 Staked map of Karous-Hjelt (G_K) profiles

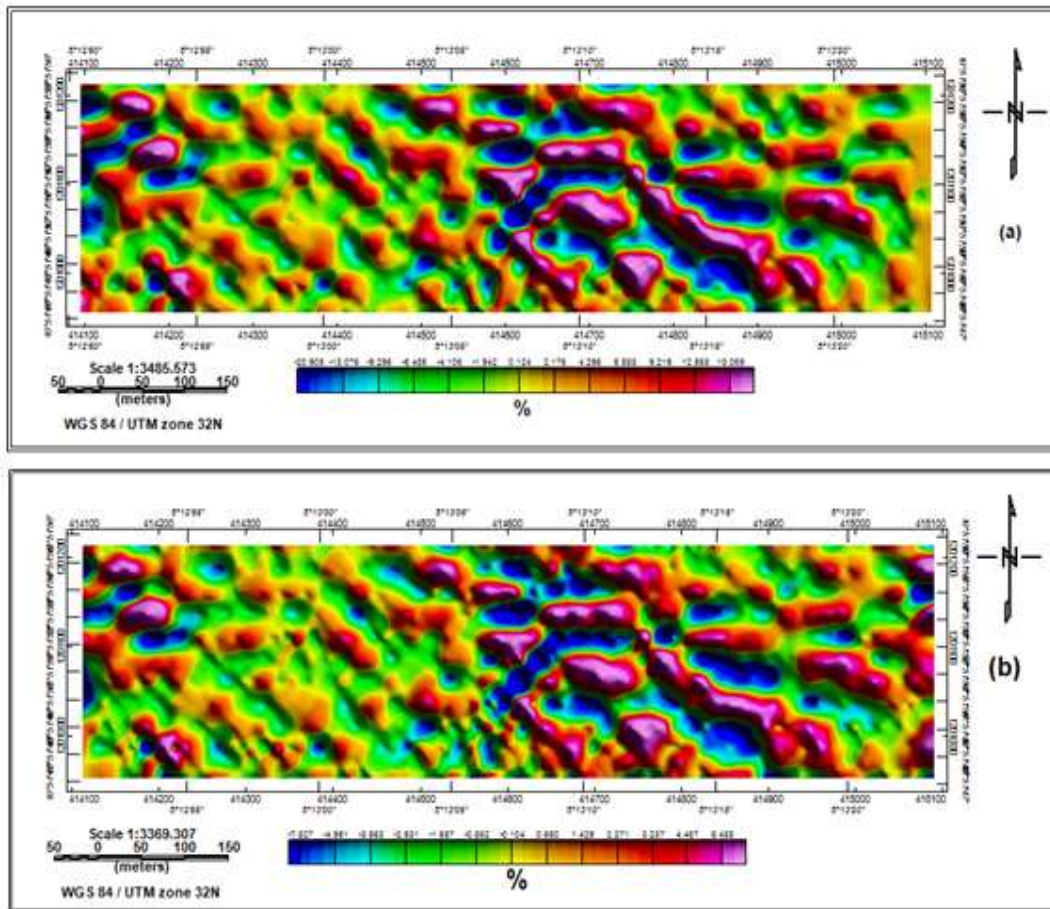Fig. 9 Raw In-phase component of all the traverses

Fig. 10 (a) Reduced to Equator of the Fraser filtered of In-phase component (b) Reduced to Equator of the Karou-Hjelt

Fig 11 shows the analytical signal map of the study area with high amplitude corresponding with the observed inferred fractures/mineralization zones in the reduced to equator of the Fraser Filtered response of the in-phase component

From the standard deviation map (Fig. 12) which is computed as the output of the reduced to equator map of the In-phase Fraser filtered, high standard deviation value was displayed by discontinuities which are related to geological structures (Fractures/ dykes/shear zones and lithological boundaries) [38].

Fig. 13 is the vectorized structural map and it shows where the structure intersects or changes direction and the areas with high prospects of mineralization [34]. The inferred geologic structures corroborate the occurrence where the Fraser filtered peaks. It can be observed that the predominant structural trend is in the NW-SE and SW-NE directions with few structures trending in the N-S direction. These structures correlate excellently well with the anomalous zones in the standard deviation. The final generated (contact occurrence density) map derived from vectorized map (Fig. 14) shows the areas (in red) with high density favorable for hosting cassiterite mineralization in the study area.
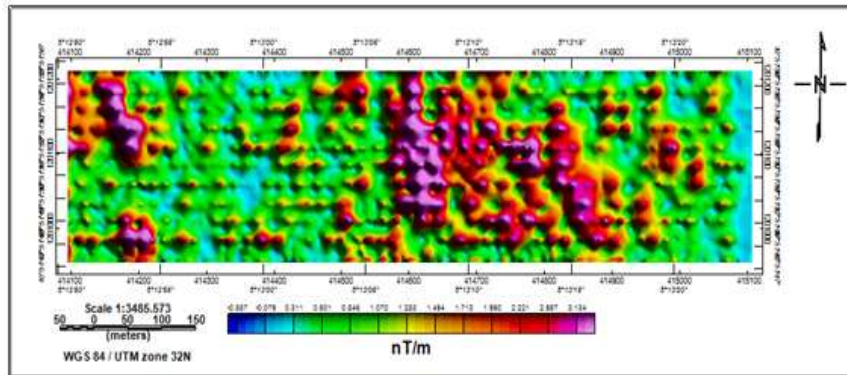

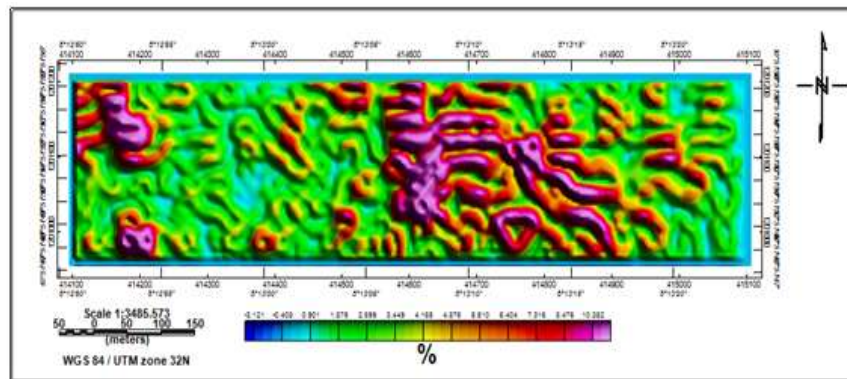Fig. 11 Analytical Signal Map

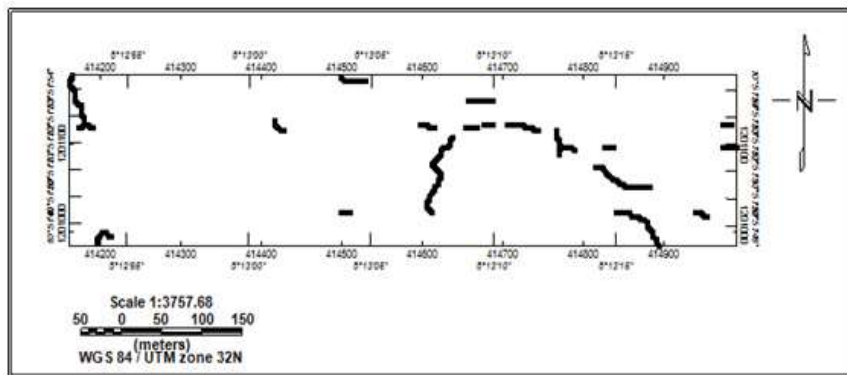Fig. 12 Standard Deviation derived from the reduced to equator map

Fig. 13 Vectorized structural map

Fig.15 shows the 2-D SPI depth estimates over the study area. The depth estimates range from - 4.9 m (shallow bodies) to – 13.7 m (deep bodies). The map shows depths > 15 m are mostly located around the southeast of the study area which corresponds to the thin conductor delineated by negative current density.

The best clustering for Euler solutions was achieved with structural index of 1, which is diagnostic of fault/ dyke model to estimate source location and depth for targets with homogenous sources. Fig. 16 show the 3-D Euler depth estimates with depth ranges greater than 15 m corresponds to the thin dip seated anomaly defined in the current density

maps found at 800 profile distances which correlate with the relatively weak conductor highlighted in the Fraser Filtered of the In-phase component (Fig 3). These inferred depths (15 m – 5 m) both from the source parameter imaging and Euler deconvolution correlate with the depths (> 9 m) reported by [1] as high cassiterite potential zones. Fig. 17 is the superposed lineament on the analytical signal map. The map shows the extracted lineament (blue) in the study area intercepts the delineated high amplitude zones which is interpreted as evidence of the occurrence and positioning of the cassiterite mineral deposits is greatly controlled by the lineament system across the study area.
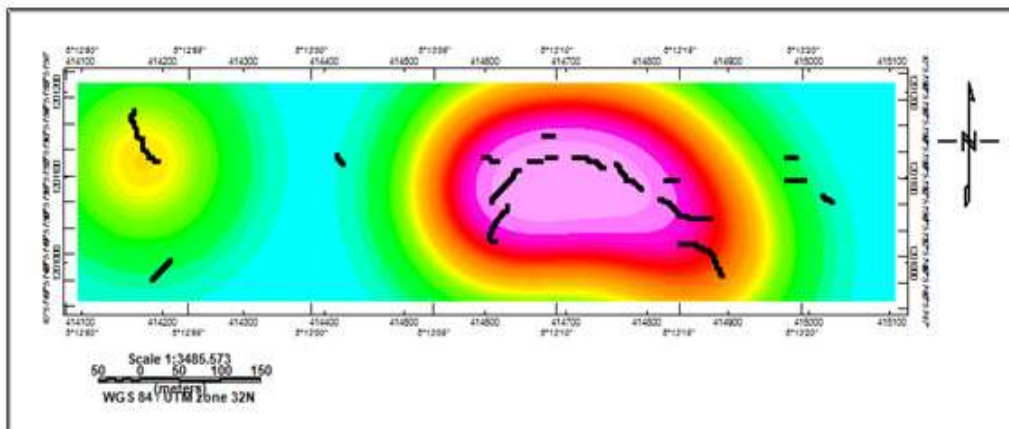

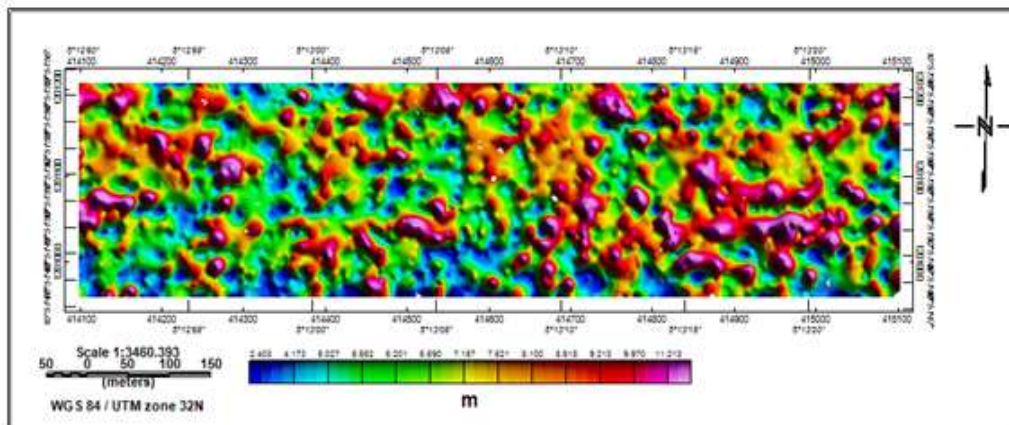Fig. 14 High density map of the study area

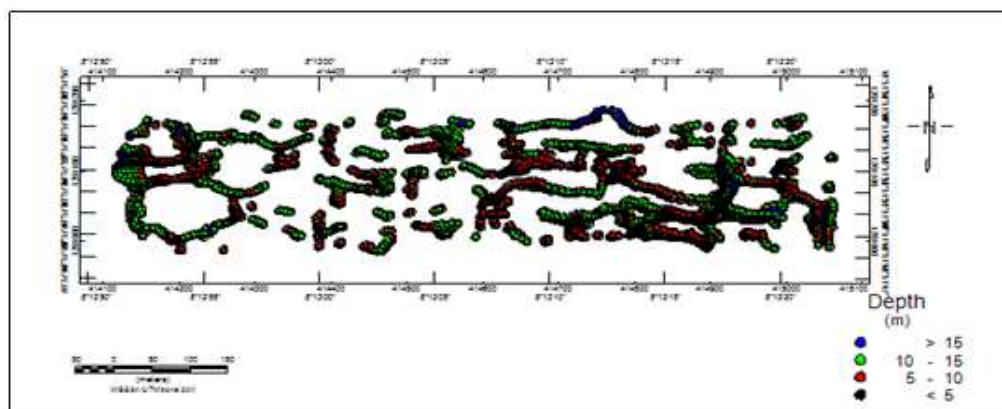Fig. 15 2D Source parameter imaging depth map of the Fraser Filtered

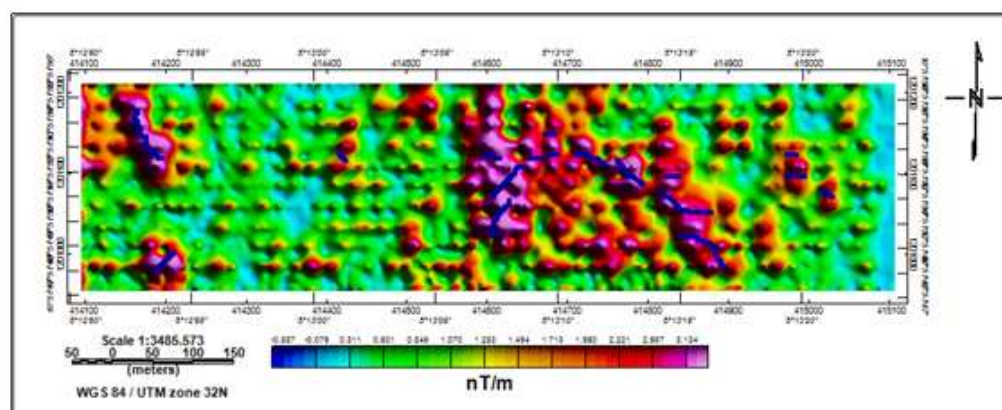Fig. 16 Euler deconvolution with structural index1 (dyke)

Fig. 17 Lineament plotted on AS MAP

IV. CONCLUSION

VLF-EM data on eleven profiles separated by 25 m with a maximum length of 1040 m were collected and processed using the Fraser and Karous-Hjelt filters and the algorithms of Oasis Montaj. The results of application of these filters on the VLF-EM data show excellent correlation. The standard deviation, the vectorized structure and the contact occurrence density algorithms of the CET were exploited and successfully delineated inferred fractures/mineralization zones from the Fraser filtered and Karous-Hjelt responses as highly favorable density zones for drilling productive cassiterite in the study area. Both the depth estimation methods (SPI and Euler deconvolution) successfully delineated zones with high mineralization potentials and the best location for drilling productive cassiterite in the study area. The occurrence and positioning of the cassiterite mineral deposits is shown to be greatly controlled by the lineament system across the study area and the development of conductive zones of high apparent current with positive values reflects inferred subsurface structural fractures and/or mineralized zones.

References

[1] M. Umar, A. L. Ahmed, S. S. Magaji and B. Bala, "Electrical resistivity investigation of subsurface topography of Rafin Bareda drainage basin as a tool for cassiterite-columbite exploration in Dutsen-Wai, Nigeria", Bayero J. of Pure and Appl. Sci., vol. 10, no. 2, pp. 209-221, 2019.

[2] C. O. Abimbola and S. A. Adedibu, "Tin Mineralization in Nigeria", Environmental and Earth Sciences Research Journal, vol. 5, no. 1, pp. 15-23, 2018.

[3] E. G. Imeokparia, "Tin Content of Biotites from the Afu Younger Granite Complex, Central, Nigeria", Economic Geology, vol. 77, pp. 710-172, 2015.

[4] J. B. Wright, "Controls of mineralization in the older and younger tin fields of Nigeria", Econ. Geol., vol. 51, pp. 303-332, 1970.

[5] A. Ebrahimi. Sundararajan and V. Ramesh Babu, "A comparative study for the source depth estimation of very low frequency electromagnetic (VLF-EM) signals. Journal of Applied Geophysics, vol. 162, pp. 174–183, 2019.

[6] N. Sundararajan, B. Procerus, S. Al-Khirbash, T. K. Al-Hosni, A. Ebrahimi, M. Al-Mashani and A. Al-Lazki, "Geophysical and geochemical investigation for structures favourable to uranium mineralization in Dhofar region, sultanate of Oman", Arab. J. Geosci., vol. 11, no. 22, pp. 700-718, 2018.

[7] N. Sundararajan, V. Ramesh Babu and A. K. Chaturvedi, "Detection of basement fractures favourable to uranium mineralization from VLF-EM signals", J. of Geophy. & Eng., vol. 2, pp. 330–340, 2011. DOI10.1088/1742-2132/8/2/018.

[8] M. N. Tijani, O. O. Osinowo and O. O. Ogedengbe, "Mapping of sub-surface fracture systems using integrated electrical resistivity profiling and VLF-EM methods: a case study of suspected gold mineralization", RMZ – Materials and Geo-environment, vol. 56, no. 4, pp. 415–436, 2009.

[9] S. I. Ibeneme, I. A. Oha, N. N. Abdulsalam and M. K. Onuoha, "Improved Mapping of the Structural Disposition of Some Younger Granite Ring Complexes of Nigeria Using High Resolution Aeromagnetic Data", J Geol. Geophy., vol. 7, pp. 443, 2018. DOI: 10.4172/2381-8719.1000443.

[10] D. E. Ajakaiye and J. F. Sweeny, "Three-dimensional gravity interpretation of the Dutsen-Wai Complex. Nigerian Younger Granite Province. Tectonophysics, Elsevier Scientific Publishing Company, Amsterdam, vol. 24, pp. 331-341, 1974.

[11] D. C. Turner, "Structure and tectonic setting of the younger granite ring complexes of Nigeria and southern Nigeria, Part I: Ring complexes and their component units", Savannah, vol. 1, pp. 223-236, 1972.

[12] R. R. E. Jacobson and W. N. Macleod, "Geology of LaRue, Banke and adjacent Younger granite ring complexes. Geological Survey of Nigeria Bulleting, vol. 33, pp. 1-117, 1977.

[13] D. C. Turner, "Ring structures in the Sara- Fiera younger granite complex, northern Nigeria", Q. J. Geol. Sot., London, vol. 119, pp. 345-366, 1963.

[14] W. N. Macleod, D.C. Turner, E.P. Wright, The geology of the Jos Plateau, General Geology Bulletin Geological Survey, Nigeria, vol. 32, pp. 118,1971.

[15] N. G. Obaje., Geology and mineral resources of Nigeria. Lecture Notes in Earth Sciences, Springer Verlag Berlin Heidelberg, vol. 120, pp. 221. https://doi.org/10.1007/978-3-540-92685 -6, 2009.

[16] J. D. McNeill and V. F. Labson, "Geological mapping using VLF radio fields", In: Nabighian, M.C. (Ed.), Geotechnical and Environmental Geophysics, Review and Tutorial, Society of Exploration, Tulsa, vol. 1, pp. 191–218, 1991.

[17] M. E. Parker, "VLF electromagnetic mapping for strand mineralization near Aberfeldy Secondhand Trans. Inst. Mining Metall, vol. 89, pp. 123–33, 1980.

[18] W. J. Phillips and W. E. Richards, "A study of the effectiveness of the VLF method for the location of narrow mineralized zones Geo-exploration, vol. 13, pp. 215–26, 1975.

[19] A. S. Saydam, "Very low frequency electromagnetic interpretation using tilt angle and ellipticity measurements", Geophysics, vol. 46, pp. 1594–606, 1981.

[20] N. Sundararajan, V. Ramesh Babu and N. P. Shiva, Y. Srinivas, "VLFPROS—a MATLAB code for processing of VLF-EM data Computer", Geoscience, vol. 32, pp. 1806–13, 2006.

[21] M. Chouteau, P. Zhang and D. Chapellier, "Computation of apparent resistivity profiles from VLF-EM data using linear filtering", Geophysics Prospect, vol. 44, pp. 215–232, 1996.

[22] Y. Jeng, M. J. Lin and C. S. Chen, "A very low frequency-electromagnetic study of the geo-environmental hazardous areas in Taiwan", Env. Geol., vol. 46, pp. 748-795, 2004.

[23] D. C. Fraser, "Contouring of VLF-EM data", Geophysics, vol. 34, pp. 958–67, 1969.

[24] R. V. Babu, S. Ram and N. Sundararajan, "Modelling and inversion of magnetic and VLF-EM data with an application to basement fractures: A case study from Raigarh, India", Geophy., vol. 72, pp. 133– 140, 2007.

[25] R. D. Ogilvy and A. C. Lee, "Interpretation of VLF-EM in-phase data using current density pseudo sections", Geophysics. Prospect, vol. 39, pp. 567–80, 1991.

[26] M. N. Nabighian, "The analytical signal of 2D magnetic bodies with polygonal cross section, its properties and use for automated anomaly interpretation", Geophysics, vol. 37, pp. 507–12, 1972.

[27] M. Karous and S. E. Hjelt, "Linear filtering of VLF dip-angle measurements", Geophy., Prospect, vol. 31, pp. 782–7, 1983.

[28] R. J. Blakely and R.W. Simpson, "Approximating edges of source bodies from magnetic or gravity anomalies, Geophy., vol. 51, pp. 1494– 1498, 1986.

[29] J. B. Thurston and R. S. Smith, "Automatic conversion of magnetic data to depth, dip, and susceptibility contrast using the SPI method", Geophy., vol. 62, pp. 807-813, 1987.

[30] K. A. Salako, E.E Udensi, Spectral Depth Analysis of part of upper Benue Trough and Bornu Basin, Northeast Nigeria, using Aeromagnetic data. Int. J. Sci. Res., vol. 2, no. 8, pp. 100-115, 2013.

[31] M. A. Al-Badani and Y. M Al-Wathafi, "Using the aeromagnetic data for mapping the basement depth and contact locations, at southern part of Tihamah region, western Yemen", Egy. J. of Pet., vol. 27, pp. 485–495, 2018.

[32] D. Core, A. Buckingham and S. Belfield, "Detailed structural analysis of magnetic data done quickly and objectively", SGEG Newsletter, 2009.

[33] E. J. Holden, M. Dentith and P. Kovesi, "Towards the automatic analysis of regional aeromagnetic data to identify regions prospective for gold deposits", Comput. Geosci., vol. 34, pp. 1505–1513, 2008.

[34] Geosoft, OASIS Montaj 8.3.3 Mapping and Processing System®, Geosoft Inc., 2015.

[35] N. K. Abdullahi and I. B. Osazuwa, "Geophysical imaging of municipal solid waste contaminant pathways", Environ Earth Sci., vol. 62, pp. 1173–1181, 2010. DOI 10.1007/s12665-010-0606-3.

[36] P. I. Olasehinde, P. C. Pal and A. E. Annor, "Aeromagnetic anomalies and structural lineaments in the Nigerian Basement Complex", J. of Af. Earth Sci. (and the Mid. E.), Vol. 11, no. 3–4, pp. 351-355, 1990.

[37] D. E. Ajakaiye, D. H. Halt, T. W. Miller, P. S. T. Verheijan, M. B Awad and S. B Ojo, "Aeromagnetic anomalies and tectonic trends in an around the Benue trough, Nigeria", Nature, vol. 20, pp. 319, 1986.

[38] A. S. M. Assan, R. A. Y. El-Qasses and M. H. M. Yousef, "Detection of prospective areas for mineralization deposits using image analysis technique of aeromagnetic data around Marsa Alam-Idfu Road, Eastern Desert, Egypt", Egy. J. of Pet., vol. 28, pp. 61–69, 2019.